

REMOTE PREDICTIVE MAPPING OF VOLCANIC TERRAIN ON EARTH AND MARS: AN ANALOG CASE STUDY IN THE CANADIAN ARCTIC. S. Lachance¹, M. Lemelin¹ and M.-C. Williamson², ¹Département de géomatique appliquée, Université de Sherbrooke, 2500 boul. de l'Université, Sherbrooke, QC, Canada, J1K 2R1, stephanie.lachance6@usherbrooke.ca; ²Département de géomatique appliquée, Université de Sherbrooke, 2500 boul. de l'Université, Sherbrooke, QC, Canada, J1K 2R1, myriam.lemelin@usherbrooke.ca; ³Geological Survey of Canada, 601 Booth St, Ottawa, ON, Canada, K1A 0E8, marie-claude.williamson@nrcan-rncan.gc.ca.

Introduction: Thematic geological maps are produced using geospatial data in a process referred to as remote predictive mapping (RPM). RPM is a tool that either helps geologists identify regions of interest for their field campaigns or serves to fill knowledge gaps in frontier regions, or both. Remote predictive maps are usually derived from supervised classifications performed on multispectral satellite images acquired in the visible, near infrared and shortwave infrared wavelengths. However, a higher spectral resolution is often sought to highlight the absorption and emission peaks that are characteristic of different minerals and rock types. Moreover, the use of a supervised classification requires *a priori* knowledge thus contradicting the underlying objective of predictive mapping.

In this research project, we seek to improve classification methods used for remote predictive mapping. The objectives are to (1) generate a remote predictive geological map using emerging satellite imagery and classification methods (i.e., PRISMA hyperspectral satellite image, the self-organizing maps method); and (2) compare our results with those obtained using traditional approaches (e.g., multispectral imagery and Random Forest).

Study Area: Located at the head of Expedition Fiord on central Axel Heiberg Island, Nunavut (Figure 1), the study area is part of the Sverdrup Basin geological province. Lithological units include clastic strata of marine and terrestrial origin, carbonate strata, evaporites and diapirs. Flood basalts and associated sills and dykes of Cretaceous age were emplaced mostly in the east-central portion of the Sverdrup Basin. They are grouped with other circum-arctic manifestations of the High Arctic Large Igneous Province (HALIP). The study area contains both gossans and paleohydrothermal deposits that are associated with HALIP igneous rocks. Gossans are visible on satellite images because of their yellow-orange colour (Figure 2). The hydrothermal system of Expedition Fiord is related to the presence of evaporite and diapirs [2]. The system could support microbial life, making it a site analogous to what could be found on Mars [1, 2].

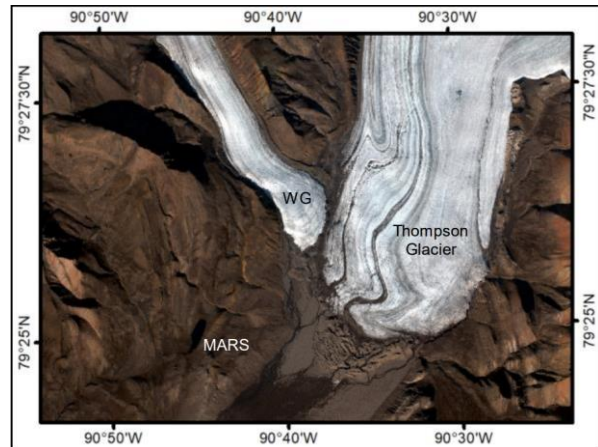


Figure 1: Location of the White Glacier (WG) analogue site at the head of Expedition Fiord, Axel Heiberg Island, Nunavut (WorldView-2 natural color composite image) [1]. The location of the McGill Arctic Research Station (MARS) is also indicated. The image is ~12 km wide.



Figure 2: WorldView-2 satellite view of gossans near MARS station. Left: Gypsum Hill Gossan, located at the south-east of the station (upper-left of the image). Right: Gossan located at the north-east of the station. The gossans are approximately and respectively 150 m and 50 m in width.

Data and method: In this research project, we compared PRISMA hyperspectral satellite images with WorldView-2 multispectral satellite images and a Radarsat-2 quad-polarization satellite image. Once the applicable corrections and enhancements methods were applied, multiple combinations of the data were used as input for the classification methods.

Classifications. The Self-Organizing Maps (SOM) method, an unsupervised artificial network, were compared to Random Forest, a frequently applied supervised classification method. Since SOM give more importance to data layers having large ranges of values [3], a data transformation is first required for this classification method to set the same range to all datasets. After initializing the grid, the best matching node in the grid is identified for each input vectors (Figure 3). The nodes' weights are updated using a neighborhood function. The previous two steps are then reiterated. After multiple iteration, the grid will take the shape of the original dataset while preserving its topological structure. Several statistics (e.g., error quantization error, topographic error) and visualization tools (e.g., u-matrix, component planes) are available to evaluate the classification results. If the number of classes (nodes in grid) is too high, another unsupervised classification method (i.e., k-means) can be applied in order to reduce it.

The sites required for the training of Random Forest were selected from a previous geological map of the area [4] and the coordinates of alterations from previous studies [5]. The transformed divergence was used to verify the separability of all pairs of classes. The sites were then divided into two groups: the training set (70%) and the validation set (30%). Before training every decision tree, two subsets of the training set were randomly selected to train the tree and evaluate it. After training all the trees, the class most frequently associated with each input vector was assigned to it. Several statistics are available to evaluate the quality of the classification (i.e., confusion matrix, f-score).

Validation. We carried out a preliminary validation of the classifications using the available 1:100 000 scale geological map of bedrock available for the Strand Fiord-Expedition Fiord area [4] with the objective of ground truthing the results during upcoming fieldwork. First, field and laboratory measurements using hyperspectral and X-ray spectrometers will be used to validate the RPM tool for mapping in volcanic terrain. Secondly, digital field mapping at a 1:10 000 scale will provide a better resolution of geological units in the vicinity of the McGill Arctic Research Station, located on the north shore of Expedition Fiord.

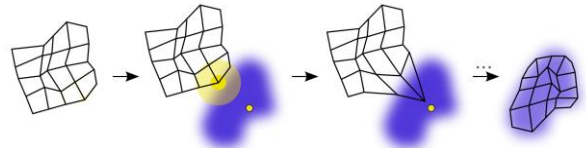


Figure 3: Four training steps of self-organizing maps [6]. From left to right: (1) The grid is initialized. (2) The best matching node is identified for each vector in the dataset. (3) The new nodes' weights are calculated. (4) The resulting grid is obtained after repeating steps (2) and (3) as much as needed.

Results: Both classification methods were implemented using IDL and python programming languages. Preliminary tests were carried out with the WorldView 2 multispectral image. While random sampling was frequently used in previous studies to initialize the nodes' weights, the results from the SOM classifications indicate that the learning process of the algorithm in this project is reduced. The classification is also influenced by the ratio between the incident angle of the sun and the slope of the ground as captured on the WorldView-2 satellite images. Topographic corrections on the WorldView-2 image appear to be the cause of this problem. The selection of training sites for Random Forest in the western sector of the study area is greatly impacted by the accumulation of sediments. Although the WorldView 2 image has a spatial resolution of 2 meters per pixel, the identification and delineation of some geological formations (e.g., intrusive rocks such as sills and dykes) were challenging because of their small size.

Conclusion: Future work will incorporate the use of a principal component analysis to improve the grid initialization for SOM. Topographic corrections for the WorldView-2 image will also be revised. Future classifications will include a mix of bands from PRISMA and Radarsat-2 images. Finally, in situ data will be acquired during fieldwork to ground truth and improve the remote predictive geological map.

References: [1] Lemelin, M. et al. (2020) *LPS LI*, Abstract #2636. [2] Zentilli, M. and al. (2019) *Geofluids*, 2019, 1-33. [3] Ponmalai, R. and Kamath, C. (2019). *Lawrence Livermore Ntl. Lab.*, 46 p. [4] Harrison, J. C. and Jackson, M.-P. (2010) *Geo. Survey of Canada*, map 2157A. [5] Clabaut, E. et al. (2020) *Rem. Sens.*, 12, 3123. [6] Modified from Stowell, D. (2010).